World Academy of Science, Engineering and Technology
International Journal of Mechanical and Industrial Engineering
Vol:18, No:5, 2024

Applications for Additive Manufacturing Technology for Reducing the Weight of Body Parts of Gas Turbine Engines

Liubov A. Magerramova, Mikhail A. Petrov, Vladimir V. Isakov, Liana A. Shcherbinina, Suren G. Gukasyan, Daniil V. Povalyukhin, Olga G. Klimova-Korsmik, Darya V. Volosevich

***Abstract*—**Aircraft engines are developing along the path of increasing resource, strength, reliability, and safety. The building of gas turbine engine body parts is a complex design and technological task. Particularly complex in the design and manufacturing are the casings of the input stages of helicopter gearboxes and central drives of aircraft engines. Traditional technologies, such as precision casting or isothermal forging, are characterized by significant limitations in parts production. For parts like housing, additive technologies guarantee spatial freedom and limitless or flexible design. This article presents the results of computational and experimental studies. These investigations justify the applicability of additive technologies (AT) to reduce the weight of aircraft housing gearbox parts by up to 32%. This is possible due to geometrical optimization compared to the classical, less flexible manufacturing methods and as-casted aircraft parts with over-insured values of safety factors. Using an example of the body of the input stage of an aircraft gearbox, visualization of the layer-by-layer manufacturing of a part based on thermal deformation was demonstrated.

***Keywords*—**Additive technologies, gas turbine engines, geometric optimization, weight reduction.

I. Introduction

THE production of low-weight body parts of gas turbine engine (GTE) and helicopter transmissions always presents significant design and technological challenges. Just as, in the challenge of increasing the efficiency and strength reliability of gas turbines, the materials and constructions of turbine blades play a key role [1], [2]. It generally applies to the design and manufacture of gear casings and other drive systems with complex configurations and significant static and dynamic loads. Dynamic loads are caused by the revolution of the rotating parts (shafts and gears) at the input stage higher than 2.0×10^4 rpm. In this case, shock and cyclic loads arising in the engagement are transmitted through the bearings to the body of the input stage. Based on the degree of perceived loads and the ratio of effective and permissible strains, the aircraft transmission body parts consist of low-loaded (safety factor $k \geq 5$) and heavy-loaded. The safety factor is at the limit of allowable values.

Today, the traditional and most common method of manufacturing body parts from alloys based on aluminum (Al), titanium (Ti), and magnesium (Mg) is complex-shaped casting [3]-[5]. The technology of as-casted body components has many significant disadvantages: low quality of castings due to gas entrapment and resulted porosity, non-metallic inclusions such as oxides, borides, nitrides etc., low surface cleanliness and low dimensional accuracy of a part, multi-operability of subsequent machining, and the long-term duration of the manufacturing process [6]-[9].

As for aviation components, increasing the main safety factor (SF) by adding extra casting factor (CF) helps to overcome the negative impact of the described disadvantages on its structural strength and match the requirements of Aviation Regulations, e.g., Russian IAC P29 [10], European EASA CS-E, FAR33. Usually, CF is equal to 1.25 to 2. This, in turn, leads to the additional weighting of the structure and additional fuel consumption. Therefore, to obtain a metallic structure with the required strength indicators in aviation by any foundry methods it is necessary to increase the wall thickness of the parts, thereby increasing reliability and increasing the weight and size characteristics.

II. Strategies for Mass Reduction

The actual problem of reducing the weight of such structures can be solved in several ways.

1) Reducing the thickness of the walls of housings or boxes and, as a consequence, increasing their load capacity. This can be applied to low-loaded drive boxes with large values of SF.
2) Application of materials with high strength characteristics, which will reduce the mass while maintaining the strength characteristics of heavily loaded structures.
3) Topological optimization with the use of modern calculation software.
4) Reducing the CF regulated by the Aviation Regulations.

It is also possible to use a combination of these methods. These methods are rarely used in practice for cast structures. The problem with applying the first method is the technological limitations associated with the impossibility to reduce the wall thickness, despite the sufficient bearing capacity.

L. A. Magerramova, V. V. Isakov, L. A. Shcherbinina, S. G. Gukasyan and D. V. Povalyukhin are with the Central Institute of Aviation Motors, Aviamotornaya st., Moscow, 111116 Russia (phone: +79035402286; e-mail: lamagerramova@mail.ru).

M. A. Petrov is with the Department "Material Forming and Additive Technologies", Faculty of Mechanical Engineering, Moscow Polytechnic University, Moscow, 115280 Russia (e-mail: m.a.petrov@mospolytech.ru).

O. G. Klimova-Korsmik and D. V. Volosevich are with the World-Class Research Center "Advanced Digital Technologies", State Marine Technical University, Saint-Petersburg, 190121 Russia (e-mail: o.klimova@ltc.ru).

The second is directly related to strength indicators, where the "removal" of the material will mean a loss of total stiffness. In this case, it is necessary to use materials with the high specific strength (force per unit area at fracture divided by its density); that is, the so-called construction quality coefficient or *CQC*. Section III of this article provides an analysis of the materials used in casting and 3D printing.

In the third method, weight reduction by performing topological optimization is limited by the technological capabilities of the traditional casting process of the thus designed complex-profile surfaces. The introduction of 3D printing technology solves this problem.

The use of the fourth method of mass reduction (by reducing the CF value) is possible only if the quality of the castings is improved which would increase the cost of the already expensive technology and make the costs comparable.

The introduction of AT allows to solve the problems mentioned above. The production of parts using 3D printing has significantly fewer technological limitations. It will enable to obtain complex-shaped surfaces and reduce the minimum thickness of the forming wall. It is possible to neglect the additional material volume by reducing safety factors, making the structure heavier while maintaining loads. The 3D printing technology provides a smaller spread of properties and higher quality half-parts. In addition, with the help of modern software, it is possible to predict the quality of the printing process and areas with potential defects.

The application of AT brings the necessary changes to existing product designs. This applies to the body parts for aircraft such as the boxes of drive units (BDU), angular (AD) and central (CD) drives, and helicopter gearboxes. The AT provides greater freedom in designing, refining, configuring, and optimizing a new design to create more efficient and less costly products in small batches and serial production [11]. The use of AT can reduce the mass of parts due, for example, reducing wall thicknesses compared to foundry production. To achieve a successful result, the components can be optimized in compliance with their production by 3D printing methods (L-PBF, EBM, DMLS etc.) [12], [13]. This article summarizes and analyzes the experience of using AT to reduce the weight of aircraft gearboxes, declaring the changes of the safety factor after weight reduction, and shows the advantages of AT compared to traditional production methods. The originality of the paper is in the introduction of the workflow and weight optimization results for body parts, for three aircraft gearbox housings, for GTEs obtained after simulation and presenting the experimental results of the as-printed parts. The theoretical laser synthesis model for lower angular drive (LAD) was presented as well.

III. The Materials Analysis

This section reviews and analyzes the alloys application for gearboxes housing production and their contribution to the weight and strength characteristics of the structure. Reducing the weight of heavy-loaded body parts while maintaining their strength properties does not lose its relevance and is evidently more and more the topic of the finite-element (FE) simulation. The complex process requires comparative studies of the strength characteristics of the original structure, its modification and strength calculation of the modified geometry, and technological studies on the applicability of AT for the production of an optimized body. Cast magnesium alloys are usually used for the production of BDU. However, the use of magnesium alloys in AT is still developing [14]-[16]. The widespread of aluminum and titanium alloys in this segment is today's state of art [17]. The most modern production technologies for thin-walled casting and AT should reduce the BDU mass. The process of manufacturing BDU enclosures requires three primary components: technological equipment, software for modeling and simulating the growing process, and metal material in the form of powder or wire. The equipment's technical characteristics and the possibilities and conditions for using the software are widely covered in various sources [11], [18]. However, there is not much information about materials acceptable for body parts in AT with a minimum weight [18]. At the same time, metallurgical companies are trying to saturate the market with metals and alloys that are in demand in the segment.

A. Aluminum Alloys for AT

The development of aluminum-based powder alloys for AT is essential, requiring special powders from experimental alloys. Therefore, the most widely used powders are AlSi10Mg silumin powder and Scalmalloy powder with Al-4.6, Mg-0.66, Sc-0.42, Zr-0.49, and Mn content, which demonstrate high technological performance in the laser powder bed fusion (L-PBF) process [19]. The AlSi10Mg alloy is of the most significant interest in manufacturing functional body parts and prototypes; it is often used in industries requiring high mechanical strength and low weight. In particular, the powder particles of the AlSi10Mg alloy with the granulometric composition D50 change from 5 to 110 μm with the following physical characteristics: bulk density 2.68 g/cm^3, thermal conductivity 130 to 190 W/(m·K), melting temperature 570 to 590 °C, and coefficient of thermal expansion 20 to 21×10^{-6} K^{-1}. The mechanical properties of the samples obtained by the additive technology of L-PBF on 3D printers from different manufacturers are different. However, each company aims to ensure the maximum properties of printed samples at an acceptable performance (4.5 to 5.0 mm^3/s). Post-processing to remove residual strains (e.g., by hot isostatic pressing or HIP) equalizes the rates of mechanical characteristics [20].

B. Magnesium Alloys

Magnesium alloys have a low density and good surface resistance in air, alkalis, and gas environments with fluorine content and mineral oils. The melting temperature of Mg is 650 °C, the tensile strength is 190 MPa, the Young's modulus is 45 GPa, and the percentage elongation is 18%. At the same time, the metal has a high damping ability (it effectively absorbs elastic vibrations), i.e., it copes with shock loads and is weakly vulnerable to resonant phenomena. Currently, the most widely used alloys in the industry are high strength ML5 and ML5p.h. However, magnesium alloys have several disadvantages. They

are significantly inferior to aluminum alloys for corrosion resistance. They are highly oxidizable in the liquid state and capable of igniting at a temperature of 400 to 550 °C, making it difficult to manufacture castings.

The casting properties of magnesium alloys are low: reduced fluidity, considerable linear shrinkage, a tendency to form shrinkable pores, and shrinkage cracks. All these disadvantages limit the possibility of reducing the weight of the product. The following processes are typically used for casting BDU bodies: die-casting and casting in sand-clay molds. The die-castings usually have weigh from 0.2 kg up to 25 kg with a wall thickness from 3 to 9 mm. The sand-clay mold castings have the weight from 0.2 to 500 kg, and the wall thickness varies from 5 to 25 mm. Therefore, the powder metallurgy of magnesium alloy granules is of commercial interest, despite some disadvantages. Thus, some company manufactures pressed products from magnesium alloy powders with high mechanical characteristics. For example, press powder samples made of alloy (P)ZR60B with 4,6% ≤ Mg ≤ 6,8%, Zn ≤ 0,45%, and Zr content, are plastically deformable at a load of more than 246 MPa, a cast alloy of the same composition at 140 to 170 MPa. Profiles pressed from the alloy powder (P)ZK62 with Mg-8%, Zn-0.5%, and Zr-2% content, have a tensile strength of 352 MPa, δ~12%. The current established industrial production of magnesium powder is suitable for additive processes using AZ91D according to American Society for Testing and Materials (ASTM) with Mg-9%, Al-0.7%, and Zn content. In this regard, the same companies adapt their own made 3D printers for the L- PBF process of magnesium samples and prototypes made of AZ91D alloy (HanaAMT). In the 1970s, the rolling, extrusion, and drawing technologies for magnesium powders manufactured by milling (designation "MPF") were developed to produce a wire with a diameter of 0.7 to 5 mm, rods with a diameter of 5 to 18 mm, strips up to 25 mm wide, tubes, corners, and other products. To reduce the cost of procurement production, several machine-building companies purchased the wire for the initial metal alloy and independently developed technologies for layer-by-layer wire surfacing to obtain blanks with a minimum allowance for subsequent mechanical processing [21].

C. Titanium Alloys

Technological foundry titanium alloys VT6L, VT20L, etc., despite their greater density compared to aluminum and magnesium alloys, have high strength and endurance limit, work for a long time at temperatures up to 400 °C are widely used in engines for manufacturing impellers, housings, intermediate supports and other parts. Table I shows the mechanical characteristics of the alloys used in computational studies, where ρ - density, σ_b - tensile strength, σ_{02} - yield point, E - modulus of elasticity, ε - percentage of elongation, h - minimal wall thickness.

As can be seen, the powder alloys used in additive manufacturing (AM) have construction quality coefficient (CQC) values higher than foundry alloys.

TABLE I
MATERIALS' CHARACTERISTICS

Alloy type	Casting (1-2-3)			Powder (4-5-6)		
	1	2	3	4	5	6
Parameter \ Alloy grade	Aluminum AK7ch	Magnesium ML9 (T6)	Titanium VT20L	Aluminum AlSi10Mg	Magnesium (P)ZR62B	Titanium VT6
ρ, g/cm^3	2.68	1.76	4.47	2.65	1.74	4.41
σ_b, MPa	180	230	770	430	352	900
σ_{02}, MPa	100	110	700	245	n/a	860
E, GPa	70	43	108	70	45	116
ε, %	1 to 4	4	5	9	12	8
h, mm	4 to 10	4 to 6	3	2	2	2
CQC, kN·m/kg	67.3	62.5	172.2	91.4	202	195

IV. MATERIAL SELECTION AND GEOMETRICAL OPTIMIZATION OF GEARBOXES HOUSINGS

Before optimizing the BDU, it is necessary to select a powder alloy and conduct strength calculations while localizing the most loaded places on the structures to analyze the capabilities of modern casting and additive manufacturing and establish geometric and technological limitations. Several case studies represent the various methods of modifying the BDU bodies. Among the well-known methods are the topological optimization (TLO) and topographic optimization (TGO), helping in generative design and giving new look for the housing parts, i.e. re-thinking procedure for estimating the critical places with the lower SF and selecting the non-homogeneous material distribution in walls.

A. Modification of Aircraft Gearboxes and Material Selection

The engineering approach for carrying out the first method of weight reduction is demonstrated in the design of the gear casings of the aircraft engine LAD, presented in Fig. 1 before modification.

Calculations in ANSYS for the stress-strain state (SSS) of the initial gear design casing showed that it is underloaded in many places of concern. Fig. 1 shows the stress and displacement fields of the initial gearbox housing. Thus, modification of the structure to remove "excess" material can be carried out in many segments. As a result, the LAD body has its own peculiarities and functions as a part of the construction process; the design zones that can be modified by changing the geometric dimensions are determined. Those zones include (I)

a massive connection strap of variable thickness converted into an element of a constant thickness that decreases by ~3 times, (II) a tidal wall thickness reduced by ~81%, and (III) the wall thickness of the bolt wells reduced to ~45%. The initial construction material was cast aluminum alloy AK7ch, in accordance with [22].

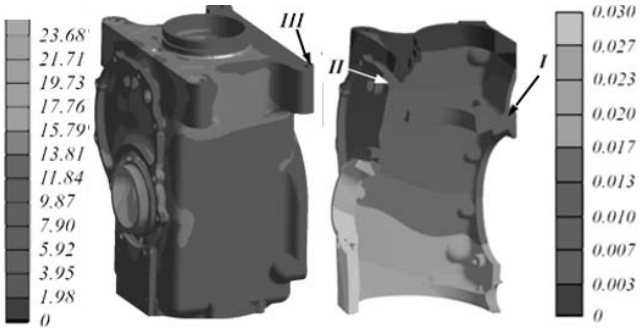

(a) (b)

Fig. 1 LAD body before modification: (a) equivalent stress (MPa) and (b) displacement (mm) fields

The comparative results of the simulation are presented in Table II, where u_{sum} – total displacement, σ_{eqv} – equivalent stress, ε_{eqv} – equivalent strain. For a modified design intended for manufacturing using AT, a casting aluminum alloy should be replaced by AlSi10Mg alloy powder. The combination of the material and structural constructional changes helps to decrease the weight of the LAD by approx. 15%. At the same time, the minimal safety margins ($SF = \sigma_{02}/\sigma_{eqv}$) were sufficient for the required (IAC, EASA) operating conditions (SF = 9.6 for AK7ch vs. SF = 5 for AlSi10Mg). However, it is practically impossible to manufacture such a design by casting because of the small thicknesses in the complexly configured areas of the part. Such a modified design fulfills the advantage features of AM technologies.

TABLE II
COMPARATIVE RESULTS FOR THE ORIGINAL AND MODIFIED DESIGN

Alloy	Initial (AK7ch), casting			Modification (AlSi10Mg), AM		
Area	σ_{eqv}, MPa	ε_{eqv}, %	u_{sum}, mm	σ_{eqv}, MPa	ε_{eqv}, %	u_{sum}, mm
I	11.95	0.0169	0.0143	48.71	0.0539	0.0354
II	14.34	0.0208	0.0081	15.72	0.0230	0.0141
III	12.30	0.0222	0.0065	14.59	0.0250	0.0088

B. Geometrical Optimization of the Gearboxes

A more significant weight reduction can be achieved based on part's geometrical optimization (GO). Now, not only in the aviation industry but also in other areas of mechanical engineering, GO methods play a significant role, help reduce structure's weight while maintaining its strength characteristics. However, manufacturing the optimized part is often impossible due to complex surfaces that cannot be produced using mechanical processing. In addition, if the part does not perceive significant loads and has extensive strength values, such as an aircraft engine drive box, the GO model has a small wall thickness, which makes it impossible to produce by casting. The volume of the removed material is, thus, limited not by the strength indicators but by the manufacturing technology. As a result, the advantages of GO are negated for parts such as airframe drive systems when trying to implement them physically.

The use of AT helps to solve the problems described above. According to the results of the analysis of the production of aviation enterprises, even when using thin and precise casting, the minimum wall thickness in the manufacture of parts made of aluminum and titanium alloys is 3 mm and in the manufacture of magnesium alloys from 4 mm. The minimum wall thickness of components produced by additive methods is 2 mm.

The descriptive part of the mathematical model for TLO and TGO for solid isotropic material with penalization function (SIMP) was mentioned by Sigmund elsewhere [23], [24]. Since that moment several proprietary software developers used it as the main model in their products (ANSYS, Altair Inspire and OptiStruct) [25], [26]. The iterative procedure is the local approximation method that determines the solution. The gradient-based optimization algorithms control the convergence of the solution, like method of feasible directions, sequential quadratic programming, etc. Additionally, the relatively new topology optimization method called level set method is used in the pointed software as well.

C. The First Example: TLO for Aircraft Gearbox

Calculations and subsequent optimization of the generator drive box housing (Fig. 2 (a)) were carried out using ANSYS software. Boundary conditions were imposed on the model: full constrained on the flange; forces simulating loading through bearing supports; loading from tightening bolts; and pressure from oil inside the housing. Standard gravity force was also applied to the model.

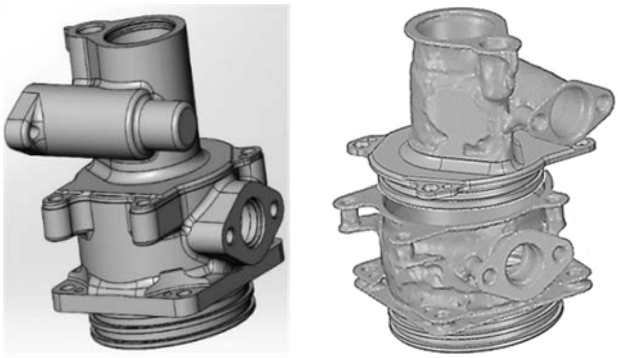

(a) (b)

Fig. 2 Original (a) and optimized (b) models of aircraft gearbox

The values of equivalent stresses and strength margins were obtained, sufficient to meet the strength conditions. To save material and due to the complexity of manufacturing parts using standard metallurgical methods, TLO was conducted to reduce mass and subsequent manufacturing using AM.

TLO was carried out using the finite element method in ANSYS based on the following assumptions:

- Structurally unchangeable elements are the entire internal geometric surface, connecting and contacting surfaces with external parts and the locations of fasteners.
- The main criterion for the calculation is the maximum reduction in the structure's mass (i.e., goal function is a mass minimization) while maintaining the required structural rigidity and strength values.
- It is necessary to perform a validation static calculation of the optimized model.

The direct optimization result is a model in the STL format, a set of triangular faces. Because such a model has many geometric inaccuracies (Fig. 2 (b)), its subsequent processing must be performed before the manufacturing stage. To prepare the model for the production stage, it is necessary to make smoothing of irregularities, removal of sharp edges, and other design operations. Model processing is often a more complex task than the rest of the optimization steps. Therefore, the final optimized design (Fig. 3) was obtained by unique manually editing the resulting model based on the optimization results for each manufacturing process.

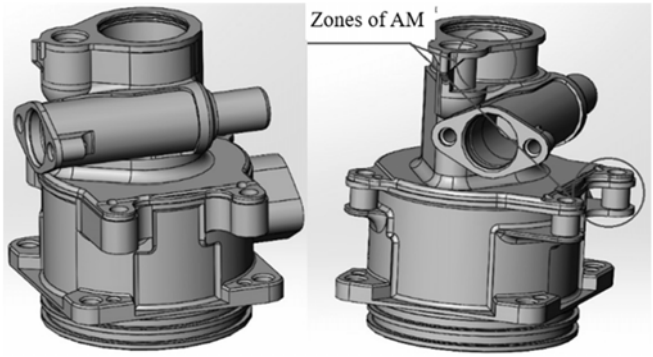

(a) (b)

Fig. 3 Models after the model's optimization for fine casting (a) and additive manufacturing (b)

The results of topological optimization can be used to reduce the mass of the cast structure incomplete in contrast to the model designed for production by any AT method. Fig. 3 (a) shows a model for manufacturing by casting. The production of an optimized model considering the zones outlined in circles in Fig. 3 (b) can only be realized by 3D printing methods. The additional weight reduction of parts with significant safety margins can also be achieved by replacing the material, for example, from a titanium to an aluminum alloy.

A similar solution was tested for the aircraft gearbox made from AlSi10Mg. While maintaining the required safety margins, an additional mass reduction of more than 5% was obtained. Another significant advantage is the reduced manufacturing cost due to cheaper aluminum powders instead of titanium. Table III shows a comparison of the weight, size, and strength characteristics of the aircraft drive body structure made of titanium alloy after TLO and refinement of the optimized design for the capabilities of AM and casting.

Optimization makes it possible to mitigate the weight of the construction by 12.3% for foundry production and by 19% for AM, keeping the high strength demands. Besides, replacing titanium alloy with aluminum alloy reduces weight by 24.8%.

TABLE III
COMPARATIVE RESULTS OF CALCULATIONS WHEN USING AT IN THE MANUFACTURE OF AN AIRCRAFT GEARBOX (BODY PART) (STRENGTH-WEIGHT-SIZE CHARACTERISTICS)

Construction alloy	Weight, kg	Max. σ_{eqv}, MPa	Weight saving, %
VT20L (conventional)	1.05	2.89	n/a
VT6 (optimized for AT)	0.85	6.5	19.0
VT20L (optimized for casting)	0.92	n/a	12.3
AlSi10Mg (optimized for AT)	0.79	7.3	24.8

D. The Second Example: TLO and TPO for LAD

For AM parts, it is necessary to use different specialized software than typically implemented in a classic computer-aided design (CAD) program, because the first one includes specific tools and equations. Shape construction must initially match the loading scheme that the part is undergoing. The known practical aspects of the geometrical optimization section allow the shape of the part to correspond to the loading scheme. Fig. 4 shows the results of geometrical optimization of three walls designated as design space of a simplified 3D model (without rounding, chamfers, etc.) of a gearbox housing, in which the main strength parameters are determined (Table IV).

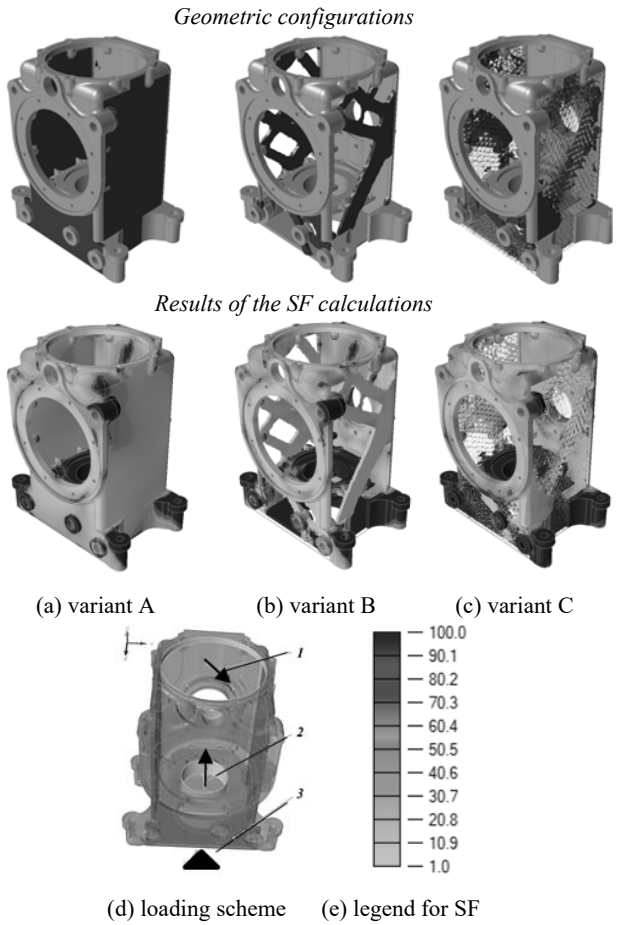

Fig. 4 Results of TLO of the gearbox housing walls

The natural vibrations were considered based on the first 10

modes. For the mesh structure, a 70% filling was considered and is a start point, at which the results could be obtained on the average desktop (Intel Core i5 10th Generation, RAM 8 GB, NVidia Quadro P620) within a relative short time (~6 hours). The search function of maximum rigidity of the part structure was selected as a target or aim function, with the possibility of reducing the material quantity up to 30%. The calculations were performed using the solidThinking Inspire software in the Structure module for the simplified loading scheme represented in Fig. 4 (d). It included forces (1) and (2) equal to 10,000 N (vector in the XOY plane, in the - OX and + OY directions, under 45°) and 1,000 N (vector in the + OX direction), respectively, as well as a full constrained degree of freedom (DOF = 0) for the bottom face (3).

The results of the safety factor (SF) calculations reduced to the same legend range are shown for three variants: before optimization for solid (variant A), topologically optimized (variant B), and lattice-optimized (variant C) geometries.

The SF was determined as a ratio of the yield stress point to the calculated stress value. The minimum value of the SF was held for critical because even the small weak area can be represented as a potential stress concentrator leading to the local or global part fracture. The highest effective stress was obtained for a solid wall and the lowest for a lattice-based wall. A similar trend was also recapitulated for the maximum value of the natural vibration frequency. Therefore, the lattice-based walls had insufficient strength at a 70% filling ratio, and the risk of failure was exceeded by ~30% (compared to SF = 1). To increase the strength characteristic of such a structure, the degree of structure filling should be higher than 70%. Further, the results of topology or lattice optimization could be used as a filling material between two solid plates with high stiffness.

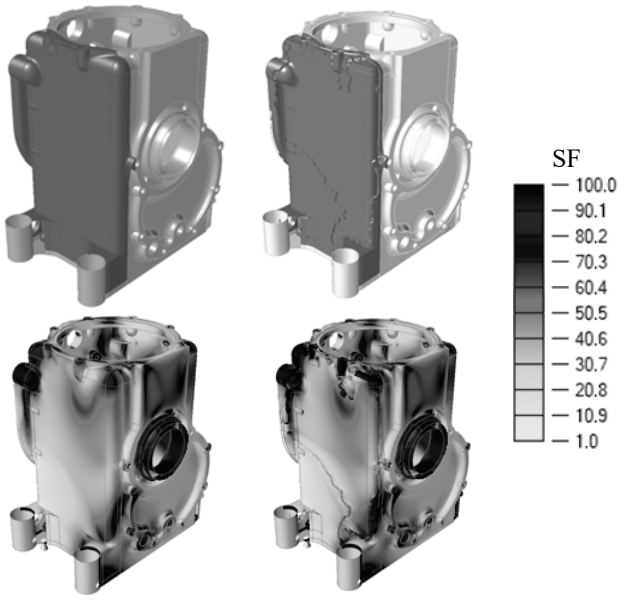

(a) initial variant (b) after optimization

Fig. 5 Results of TGO (variant D)

The problem of TGO or placing stiffening ribs was considered separately (Fig. 5). Solution of this task can help increase the strength and frequency characteristics of the gearbox housing walls. One of the three walls free of ribs was considered. The stiffening ribs are distinguished by a discrete arrangement in the design space and the circumscribed perimeter.

According to the results (Fig. 5, Table IV), the topographic optimization (variant D) was slightly inferior to the topological optimization (variant B) in terms of natural vibration frequency and effective stress values.

TABLE IV
RESULTS OF THE CALCULATED STRENGTH PROPERTIES OF THE GEARBOX HOUSING FOR OPTIMIZATION PROBLEMS

Variant	Effective equivalent stress, MPa		Natural frequency	Strain energy	Safety factor	
	min, 10^{-6}	*max, 10^{2}*	*max*	*max, 10^{5}*	*min*	*max, 10^{7}*
A	376.30	1.17	3 625	1.82	2.06	0.06
B	5.44	1.26	2 556	0.30	1.91	4.44
C	80.86	3.53	2 292	1.75	0.68	0.30
D	0	1.40	2 498	0.07	1.73	2.58

V. AT IN THE PRODUCTION OF HELICOPTER GEARBOXES

As mentioned above, another method of reducing the weight of hull parts is to reduce the extra CF regulated by §29.621 of the Aviation Regulations relating to transport category helicopters. The value of the extra SF varies in the range of 1.25 to 2 or more depending on the casting quality of the blanks and methods of its control. In addition, for those critical castings, the extra CF, which is less than 1.5, requires testing of three samples, which need additional expenses.

Increased requirements are imposed on the body parts of the helicopter gearboxes compared to the drive system of civil aviation engines since the latter are not the main parts critical to the consequences of failures. In order to mitigate these requirements, a manufacturing technology should be used in which the dispersion of mechanical characteristics should be minimal and their value maximized compared to casting. Numerical modeling of the 3D printing process helps to predict defects localization with analyzing their prevention, and perform a forecast of prototype's properties as well. The application of such an approach has been proven on the body of the experimental input stage of a helicopter gearbox.

The prototype printed case was made with an aluminum alloy powder with a chemical composition following DIN EN 1706 AlSi10M on a 3D Systems ProX DMP 320 printer. The prototype showed the following defects: shedding the joint plane's surface and a crack in the support area, critical and not permissible (Fig. 6). The first defect was most likely associated with the incorrect location of the supports, and the second with warping and the effect of high residual stresses.

The nature of such defects is caused by the following reasons that occur during the 3D printing process: High residual temperature strains can lead to shape distortion (warping), especially of thin-walled parts during construction and after removal from the base and removal of supports, the formation of cracks. A collision with the powder leveling device (recounter) due to deformations in the vertical direction can

lead to the formation of voids, damage to the part, powder leveler (recoater). In the worst case, the machine breaks down and stops printing the part. Defects in the part can occur due to changes in the structure and thickness of the powder layers and warping of the component. The formation of cracks in the supports of the part model (large angles of inclination of the surfaces to the horizontal and incorrect selection and installation of supports) can lead to powder shedding and, consequently, a defect in the shape of the part.

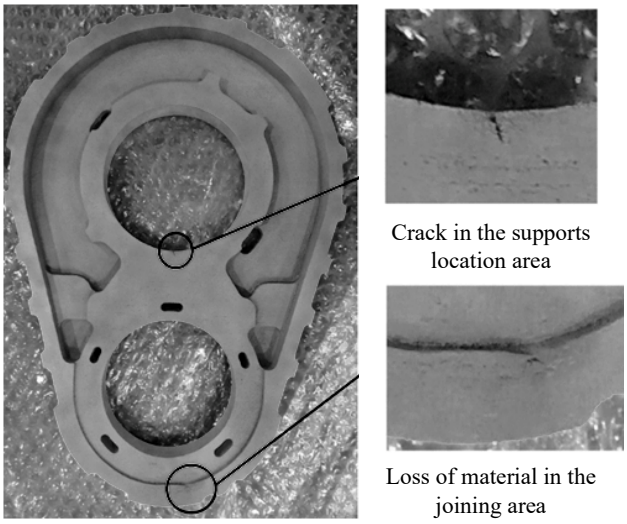

Fig. 6 Cover of helicopter gearbox with defects

In addition, as a result of layered AT, an anisotropy of mechanical characteristics appears in the constructed part, and there are residual temperature strains that affect these characteristics. A way to overcome the problem of additive manufacturing is preliminary numerical modeling. Numerical modeling of 3D printing processes is performed in several stages.

- Preparation of a 3D model: At this stage, the geometric shape of the part model (wall thicknesses, angles, etc.) is analyzed and changed if necessary.
- Layout of the part in the space of the 3D working camera.
- Preparation of construction supports: Determining the areas for which support, selecting the type, and creating support structures are required.

Development of a construction strategy (filling strategy, scanning step, layer thickness, scanning section length, section rotation angle, scanning speed) and determination of optimal characteristics (laser power, focal length, laser beam diameter in focus, and recoater speed) ensures maximum surface quality, detail density.

Analysis of critical data for industrial production like reproducibility, quality control etc., and cost estimating is required.

Modeling was conducted based on various optimization criteria. The input data for the analysis were a 3D solid-state model of the part, process characteristics, powder properties (fluidity, solidness, percentage of gas inclusions), and particle size distribution. Modeling the printing process of an aircraft gearbox was carried out using thermal deformation, which allows the effects of accumulation of deformations due to cyclic heating to be considered and provides the greatest accuracy in modeling the additive manufacturing process. Still, it is the least productive and requires the most time compared to the casting or forming processes. The algorithm assigns a base strain to each location in the part as it hardens. Every time a component is heated above the temperature threshold of 0.4 of its absolute melting point, there is an increase in strains at this point. If the part is re-melted, the strain is reset to zero. The more times a part is heated above the threshold without melting, the more stress accumulates. After the strain is calculated for each location, it is passed to the solver and applied as an anisotropic strain based on the local strain value and the local laser beam position.

The calculations reveal the most significant levels of stress and displacement distributions, occurred in the area with support structures, resulting the crack formation. On the surface with shedding, the sharp local changes in residual strains were recognized.

At last, a compensated geometric shape was obtained during 3D printing. When analyzing the initial and optimized geometric shapes (Fig. 7), the greatest discrepancy was observed between them on the periphery and in the support areas where a crack was located. Thus, modeling of additive manufacturing processes is necessary for:

- Predicting problems to solve.
- Visualizing deformations and stresses.
- Mirror compensation of occurred deformations to prevent the warpages during and after the real 3D printing.
- Protecting the printer from damage.
- Forecasting of warping.

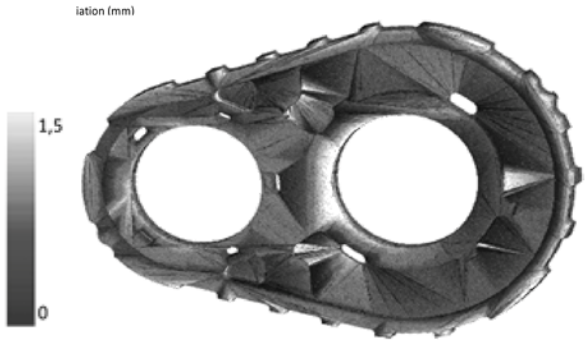

Fig. 7 Comparison of initial and optimized models

Based on the visualization of the process of layer-by-layer manufacturing of the part, the specialist can assess how the expected warping and residual stresses affect the part's final shape. The specialist can also choose the appropriate orientation of the product in the construction chamber and ways of placing supports. That helps to keep minimal required SF values without adding extra values.

VI. Simulation of the Synthesis Process of the LAD Gearbox Housing

As a criterion for using the additive manufacturing method

for body parts, it is convenient to use the trinity of characteristics "productivity – manufacturing accuracy – strength properties." In contrast to the dual criterion of the "black-white" type, in such a triad criterion, one of the characteristics (the primary one) acts as an arbitrator for the other two, which are mutually complementary. Without considering the triad, the productivity and accuracy of manufacturing parts through 3D formation are perceived as opposite concepts. There can be high accuracy and a lack of performance. In achieving performance, they do not expect high accuracy. However, the contradiction is resolved when the printing process is oriented to obtain the required strength properties, enough to endure the loads or stresses during exploitation [27].

The process of laser additive 3D formation of parts from metal powder composition (MPC) is determined by many factors. The analysis and systematization of significant factors allow to assume that among the many variables acting in the laser technology system, only a few essential, so-called order characteristics are determined, to which the rest are adjusted. These are energy-thermal characteristics.

A. Energy Thermal Calculation

According to the reported results in [28], the local powder melting in the zone of laser exposure to a dispersed medium occurs in a small range of radiation power density (intensity, I_0). At a higher laser beam power density in the heating zone, the melting of powder particles occurs. However, a plasma torch forms, negatively affecting the kinetics of the melting process. A decrease in the power density below 10^8 W/m^2 leads to a loss of uniformity in the powder melt and the appearance of teardrop-shaped discontinuities in the formed layer. Therefore, the condition $10^8 \le I_0 \le 10^{10}$ [W/m^2] should be fulfilled for optimal radiation power density in the heating spot to avoid instabilities and defects. The intensity I_0 of the radiation incident on the irradiated surface is determined through the power of the laser beam W and the area of the focus spot with a diameter d as in (1).

At the same time, the duration of heating of the powder substance corresponds to the time constant τ, representing the exposure time, when the laser radiation passes through a specific point on the surface at a scanning speed v. Since the radiation is focused on a spot with a diameter d the time constant calculates as in (2).

Based on the optical absorption coefficient α, the thermal effect of the laser beam on the powder can be represented as a surface source with a power density as in (3), acting for a time τ. During this period, the wave of thermal conductivity will spread into the powder layer to a depth of z. Heat transfer in a powder medium has its own characteristics since the bulk density of the powder, and the size and shape of the powder particles determine the thermophysical characteristics of the desired dispersed medium. In this regard, a method for averaging the thermophysical characteristics of aluminum powder is proposed in [29]. The method is based on the obvious fact that the thermal conductivity of a material depends on its porosity. With increasing porosity, the thermal conductivity of the material decreases, since the pores contain air, the thermal conductivity which is small and is only 0.024 W/(m·°C).

Let us assume that, the relationship between the characteristics of the thermal conductivity, heat capacity, and density for the solid, compacted material (λ, C, ρ) and discrete, powder material (λ', C', ρ') are proportional to the coefficient 1/ε; therefore, following relationships can be obtained: $\lambda = (1/\varepsilon)\lambda', C = (1/\varepsilon)C', \rho = (1/\varepsilon)\rho'$. During layer-by-layer laser melting process, the heat transfer process can be considered within the framework of a single linear approximation along the prototype's growing direction (OZ-axis) without taking into consideration the temperature dependencies of such characteristics like α, ε, λ', C', ρ'; therefore, the average value of the heat diffusion coefficient for the powder can be calculated as in (4). Here, the height of the molten layer z will be determined according to (5). The amount of the absorbed power is equal to power, required for powder melting. The rest power dissipates through the layers into the deep of the powder bed because of thermal conductivity; therefore, the power density can be represented as in (6). And at last, the required laser power W is calculated based on the powder melting point and either the exposure time or the height of the molten layer.

$$I_0 = 4W/(\pi d^2) \tag{1}$$

$$\tau = d/v \tag{2}$$

$$W_L = \alpha I_0 \tag{3}$$

$$k' = \lambda'/(C'\rho') \tag{4}$$

$$z = 2\sqrt{\tau k'} \tag{5}$$

$$W_L = \lambda' T/(2\sqrt{\tau k'}) \tag{6}$$

B. Optimization of Laser Synthesis Modes

As a criterion for increasing the energy efficiency of the laser L-PBF, it is reasonable to use the value of the specific energy input depending on the laser power W, speed v, and scanning step b determined as in (7). This expression is easy to compare with the known operating parameters [30] since the value of b is based on previous experiments. At the same time, the laser beam power and scanning rate are inversely proportional to each other. In the steady-state building mode, it is convenient to optimize the L-PBF process using a dimensionless similarity criterion Pe (similarly to the Peclet criterion), which characterizes the rate of laser energy introduction relative to its dissipation rate during laser working as in (8).

$$E_y = W/(vb) \tag{7}$$

$$Pe = v\sqrt{db}/k' \le 1 \tag{8}$$

The following values of the thermophysical characteristics of the AlSi10Mg powder considering its bulk density were used:

- Thermal conductivity, W/(m·°C): λ = 114 and $\boldsymbol{\lambda}'$ = 96.9.
- Melting interval, °C: ΔT = 780 to 800.
- Density, kg/m^3: ρ = 2 800, ρ' = 2 380.
- Specific heat, J/(kg·°C): C = 1.05, C' = 0.89.

Only laser power W, scanning rate v, and scanning step b were discretely changed. Based on the methodology above, the technological regimes of layer-by-layer synthesis of the gearbox housing were optimized (α = 0.8):

- Laser (beam) power, W: W = 200 to 400.
- Spot diameter, m: d = (0.08 to 0.1)·10^{-3}.
- Power density, W/m^2: $W_L = 6.3 \times 10^7$.
- Scanning rate (also known as beam travel speed), m/s: v = (2 to 6) ×10^{-3}.

C. Simulation of the L-PBF Process

FE-simulation of the L-PBF-based 3D printing process was carried out using the solidThinking Inspire software (module Print3D) [31]. The operating parameters were taken from the default settings of the 3D printer. The goal of the analysis was to fix the possible warpage before the actual 3D printing stage. The thermomechanical task formulation was applied. The pre-processing consists of several steps: machine and material selection, orienting the part on the base plate of the printing chamber, selecting the type and generating the support structures, entering the primary values of the 3D printer's parameter, and slicing the model. Fig. 8 shows the distribution and values of the temperature field from the side of the maximum values (a), the field of von Mises stresses (b), and displacements (c) in a virtual chamber. The most displaced points were allocated near the placing of four bolts that resolve the stresses in the lower part of the prototype. Therefore, the more rigid support structures of the fence type were used during 3D printing that helped to reduce the detected displacements more than three times. These images corresponded to the final stage of the 3D printing simulation of the gearbox housing when 100% of the volume of layer-by-layer calculations was performed.

The gearbox housing was manufactured of AlSi10Mg alloy powder on the 3D printer ProXDMP320 equipped with a 400 W fiber laser.

Considering the optimal Peclet criterion, parameters such as focal length (400 mm), laser spot diameter d (60 μm), powder feed ratio (400%), recoater speed (115 mm/s), and layer thickness (30 μm) were set to constant values. Fig. 9 shows a gear housing produced by 3D laser printing with a minimized mass made of AlSi10Mg alloy powder.

The metallographic microstructure of the synthesized alloy of the AlSi10Mg system was investigated elsewhere [32]. In optical resolution, the macrostructure has a form characteristic of 3D printing. According to the results of the electron backscatter diffraction (EBSD) analysis, presented on [32], the columnar grains are predominantly oriented in the 001 direction. The grain size is 5 to 25 μm.

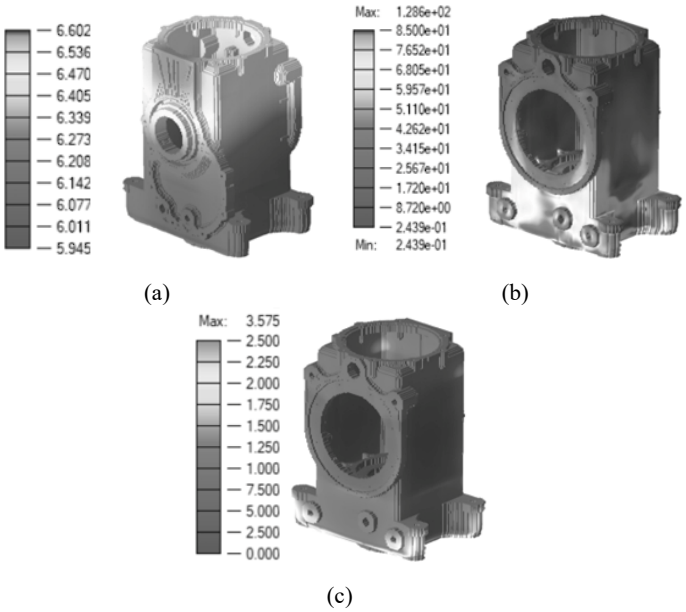

Fig. 8 Outputs (a) temperature, ×10^2 in (K), (b) equivalent stresses (MPa) and (c) displacements (mm)

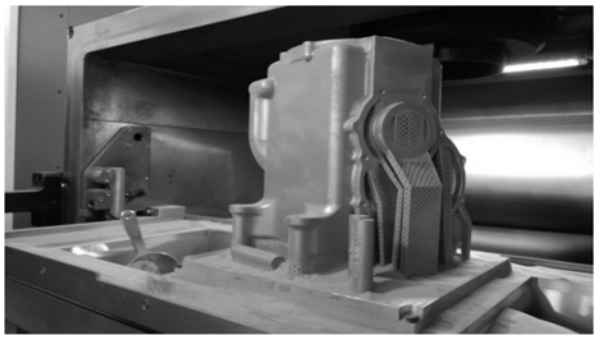

Fig. 9 Prototype of a GTE gearbox housing, made from AlSi10Mg alloy powder

VII. Results and Discussion

Using the examples of several gear casing designs, various modifications were made, which made it possible to reduce their weight.

- TLO of structures made of cast alloys was conducted. The reduction in the mass of the 3D titanium models adapted for foundry production was 12.3%.
- When manufacturing them using AT methods from magnesium and titanium alloys with a minimum wall thickness of 2 mm, it is possible to achieve a weight reduction of at least 15% while maintaining strength characteristics that meet the strength requirements. An even more significant decrease in the weight of the cases to 24.8% was achieved by replacing the titanium alloy with aluminum.
- Based on engineering approaches, the modification of the LAD case was performed. A powder aluminum alloy of the Al – Si – Mg system was selected for its production. The process of laser synthesis obtained properties of part superior to one from the foundry aluminum alloy. The

parameters of laser synthesis were optimized.

- Using the example of the body at the input stage of an aircraft gearbox, visualization of the layer-by-layer manufacturing of a part based on thermal deformation was demonstrated. As a result, the orientation of the product in the construction chamber was modified, including the method for placing of support.

The present article deals mainly with technical aspects, without analyzing the economic, time, and environmental impacts of the technology, which should be the subject of a separate study.

Despite several disadvantages of L- PBF (limitation of product dimensions, increased manufacturing time for building procedure, high expenses for mass production, the need for quality control of the powder particles after each building procedure because of deterioration of powder flow properties, and design of support and heat sink structures), preliminary studies, analysis, and observations show the advantage of AT over casting production:

- AT production is less harmful because it is done in enclosed machines without direct human involvement;
- ATs have less production waste compared to castings;
- Parts produced by the AT method require less subsequent machining and other post-treatment operations, which saves time and makes production cheaper;
- The reduction in the weight of parts obtained through the use of AT allows increasing the load capacity of the aircraft or increasing its specific characteristics, which has a favorable impact on the economic indicators.

VIII. Conclusion

Existing methods of reducing the weight of body parts of aircraft gearboxes and gearboxes are becoming the most effective when using additive technologies or AT. The use of AT, considering the topological optimization or TLO, and sequential visualization with optimization of technological parameter for processes of laser synthesis, gives an overview of prospective technological chain of preparing, planning and performing of digital precision production of a complex and integrated parts such gear casings or other aircraft components and structures.

References

[1] Geetika, S., Rayapati, S., Subrata, M. Comparison and selection of suitable materials applicable for gas turbine blades, *Materials Today: Proceedings, Vol. 46, Part 17, pp. 8864–8870 (2021). https://doi.org/10.1016/j.matpr.2021.05.003*

[2] Swain, B., Mallick, P., Patel, S., Roshan, R., Mohapatra, S., Bhuyan, S., Priyadarshini M., Behera, B. et al. "Failure analysis and materials development of gas turbine blades", *Materials Today: Proceedings, Vol. 33, Part 8, pp. 5143–5146 (2020). https://doi.org/10.1016/j.matpr.2020.02.859*

[3] Yuan, G., Li, Y., Zhou, X., Hu, L. Preparation of complex shaped aluminum foam by a novel casting-foaming method, *Materials Letters, Vol. 293, 129673 (2021). https://doi.org/10.1016/j.matlet.2021.129673*

[4] Hao, J., Yu, B., Bian, J., Zheng, L., Nie, S., Li, R. Comparison of the semisolid squeeze casting and gravity casting process on the precipitation behavior and mechanical properties of the Al-Si-Cu-Mg alloy, *Materials Characterization, Vol. 180, 111404 (2021). https://doi.org/10.1016/j.matchar.2021.111404*

[5] Ghiaasiaan, R., Amirkhiz, B.S., Shankar, S. Quantitative metallography of precipitating and secondary phases after strengthening treatment of net shaped casting of Al-Zn-Mg-Cu (7000) alloys. *Materials Science and Engineering: A, Vol. 698, pp. 206–217 (2017). https://doi.org/10.1016/j.msea.2017.05.047*

[6] Li, Y., Liu, J., Zhang, Q., Huang, W. Casting defects and microstructure distribution characteristics of aluminum alloy cylinder head with complex structure, *Materials Today Communications, Vol. 27, 102416, pp. (2021). https://doi.org/10.1016/j.mtcomm.2021.102416*

[7] Mayer, H., Papakyriacou, M., Zettl, B., Stanzl-Tschegg, S. Influence of porosity on the fatigue limit of die cast magnesium and aluminium alloys, *International Journal of Fatigue, V. 25, Issue 3, pp. 245–256 (2003). https://doi.org/10.1016/S0142-1123(02)00054-3*

[8] Wang, Q., Apelian, D., Lados, D. Fatigue behavior of A356-T6 aluminum cast alloys. Part I. Effect of casting defects, *Journal of Light Metals, Vol. 1, Issue 1, pp. 73–84 (2001). https://doi.org/10.1016/S1471-5317(00)00008-0*

[9] Yi, J., Gao, Y., Lee, P. et al. Scatter in fatigue life due to effects of porosity in cast A356-T6 aluminum-silicon alloys, *Metall Mater Trans A, Vol. 34, 1879 (2003). https://doi.org/10.1007/s11661-003- 0153-6*

[10] Code of Federal Regulations, 14 CFR, Part 29.621 Airworthiness Standards: Transport Category Rotorcraft. *https://www.ecfr.gov/current/title-14/chapter-I/subchapter-C/part-29, last amended 20/03/2022*

[11] Gibson, Ya., Rosen, D., Stucker, B., Khorasani, M. Additive manufacturing technologies, *3rd edition, Springer Nature, Switzerland, p. 698, 2021. https://doi.org/10.1007/978-3-030-56127-7*

[12] Zhao, T., Wang, Y., Xu, T., Bakir, M., et al. Some factors affecting porosity in directed energy deposition of AlMgScZr-alloys, *Optics & Laser Technology, Vol. 143 (2021). https://doi.org/10.1016/j.optlastec.2021.107337*

[13] Spierings, A., Dawson, K., Uggowitzer, P., Wegener, K. Influence of SLM scan-speed on microstructure, precipitation of Al3Sc particles and mechanical properties in Sc- and Zr-modified Al-Mg alloys, *Materials & Design, Vol. 140, pp. 134–143 (2018). https://doi.org/10.1016/j.matdes.2017.11.053*

[14] *Burmistrov, M., Magerramova, L., Grachev, D., Kozin, S., Isakov, V. Application of selective laser melting technology for printing lightweight housing parts from powder magnesium alloy for gas turbine engines, Proceedings ICAM- 2020, Moscow, Russia, May 18–21, pp. 573–575 (2021). ISBN 978-5-94049-053-1*

[15] Wessel, W., Smit, M., Al-Hamdanic, K. Clarec, A. Laser powder bed fusion of a Magnesium-SiC metal matrix composite. *Proc. CIRP. Vol. 81, pp. 506–511 (2019). URL: https://doi.org/10.1016/j.procir.2019.03.137*

[16] Liu, S., Guo, H.-J. A Review of SLMed Magnesium Alloys*: Processing, Properties, Alloying Elements and Postprocessing. J. Metals, 10, 1073, pp 1–48 (2020). https://doi.org/10.3390/met10081073*

[17] Samuel, A., Zedan, Y., Doty, H., Songmene, V., Samuel, F. A Review Srudy on the Main Sources of Porosity in Al-Si Cast Alloys. *Advances in Materials Science and Engineering, Vol. 2021, 1921603 (2021). https://doi.org/10.1155/2021/1921603*

[18] Morgunov, Yu., Saushkin, B. Additive technologies for aerospace engineering. *Additive Technologies, No. 1. pp. 30–38, 2016*

[19] Moghimian, P., Poirié, T., Habibnejad-Korayem, M., et al. Metal powders in additive manufacturing: A review on reusability and recyclability of common titanium, nickel and aluminum alloys. *Additive Manufacturing, Vol. 43, 102017 (2021). https://doi.org/10.1016/j.addma.2021.102017*

[20] Metal powders of aluminum, magnesium, titanium and silicon. Consumer properties and applications. *Edited by the Member of the Faculty of the Russian Academy of Sciences, Prof. Rudsky, A. St. Petersburg: Publishing house of the Polytechnic University. un-ta, 356 p., 2012*

[21] Frank, S., Gneiger, S., Neunteufl, E. Wire based additive manufacturing of Mg alloys, *76th Annual IMA World Magnesium Conference, Budapest, Hungary, 2019. Available online: https://www.researchgate.net/publication/336022175, last amended 23/03/2022*

[22] GOST 1783-93 «Aluminium casting alloys. Specifications», *1993*

[23] Sigmund, O. A 99 line topology optimization code written in Matlab. *Structural and Multidisciplinary Optimization, Vol. 21, pp. 120–127 (2001). https://doi.org/10.1007/s001580050176*

[24] Sigmund, O., Maute, K. Topology optimization approaches, *Structural and Multidisciplinary Optimization, Vol. 48, pp. 1031–1055 (2013). https://doi.org/10.1007/s00158-013-0978-6*

[25] Altair HyperWorks User Guide, *2021. Available online: https://community.altair.com/community?id =*

altair_product_documentation, last amended 23/03/2022

[26] Tyflopoulos, E., Steinert, M. A Comparative Study of the Application of Different Commercial Software for Topology Optimization. *Applied Sciences, Vol. 12, 611 (2022). https://doi.org/10.3390/app12020611*

[27] Isakov, V. Optimization of the technological process of laser processing from the standpoint of system-synergetic analysis. *Izvestia of MSTU, No. 2 (12), pp. 134–139 (2011).*

[28] Rykalin, N., Uglov, A., Zuev, I., Kokora, A. Laser and electron-beam processing of materials. *Moscow: Mashinostroenie, USSR, 1985, p. 496.*

[29] Ankudinov, V., Krivilev, M. Theoretical analysis of the dependence of thermophysical characteristics on porosity. *The Bulletin of the Udmurt University/ Physics, Chemistry, Vol. 4, pp. 3–8 (2012).*

[30] Dynin, N., Zavodov, A., Oglodkov M., Khasikov, D. Influence of the parameters of the selective laser fusion process on the structure of the aluminum alloy of the Al–Si– Mg system. *Proceedings of VIAM: electron. scientific and technical journal, Vol. 10(58), 2017.*

[31] Altair University, *2021. Available online: https://altairuniversity.com/inspire-3dprint-2/, last amended 23/03/2022*

[32] Magerramova L., Isakov V., Shcherbinina L., Gukasyan S., Petrov M., Povalyukhin D., Volosevich D., Klimova-Korsmik O. Design, simulation and optimization of an additive laser-based manufacturing process for gearbox housing with reduced weight made from AlSi10Mg alloy. *Metals 2022, 12(1), 67; https://doi.org/10.3390/met12010067*